Chapter 7

VACUUM SYSTEM

7.1 Introduction

Beam stability and beam lifetime are the major requirements for good operation of the synchrotron light sources. Pressures in the range of low 10^{-9} mbar are typical values to be achieved during operation in order to have a good beam lifetime; the pressure inside the vacuum chamber is produced by the thermal desorption and the photon stimulated desorption processes, the interaction between the electron beam with the residual gases leads to an elastic and inelastic scattering causing electron loses and reducing the lifetime of the beam.

To achieve the required values of the pressure, a good vacuum system need to be designed; good and efficient pumping system, good monitoring, good choice of vacuum chamber design and materials and an efficient cleaning and conditioning all will lead to low outgassing and low pressure.

7.2 SESAME Parameters

General characteristics of the machine, which are the most important from vacuum point of view, are shown in table (7.1):

Table 7.1: SESAME main parameters.

Beam energy (GeV)	2.5
Maximum beam current (mA)	400
Horizontal emittance (nm.rad)	26.596
Number of dipoles	16
Circumference (m)	128.4
Bending radius (m)	5.85193
Dipole magnetic length (m)	2.29805
Dipole magnetic field (T)	1.425
Electron beam vacuum chamber vertical / horizontal aperture (mm)	30 / 70
Distance between two dipoles LSS / SSS (m)	5.994 / 5.46

Others like photon flux, average pressure…etc will be calculated later on.

7.3 Requirements

The vacuum system must be designed in a way, which will guarantee that the following requirements must be taken into consideration:

- An average dynamic pressure of $1 \cdot 10^{-9}$ mbar must be achieved by the end of the conditioning stage, such a value for the pressure will allow a good beam lifetime of not less than 14 hours to be obtained. Good optimisation of the locations and the sizes of the pumps will assure that such values of pressure to be achieved.
- The electron beam must see a smooth surface to avoid the interaction of the electromagnetic field of the electron beam with the vacuum chamber walls, as this will produce wake fields which are sources of energy spread and sometimes killing the beam, hence the electrical impedance of the vacuum chamber must kept minimal and constant around the ring.
- Sufficient cooling, to dissipate the heat load associated with the synchrotron radiation as high power in the vacuum chamber walls will enhance thermal desorption and will

increase photon induced desorption, also the high power will cause thermal expansion of the vacuum chamber. Sufficient cooling will be by the good design of the crotch absorbers as well of the distributed absorbers.

- The physicists' requirements must be considered during the design, like small vertical dimension of the vacuum chamber to get a small distance between the magnet poles, another requirement is (and as mentioned before) an electrical continuity to avoid the RF resonance.
- Good and sufficient monitoring is required as achieving the required pressure is as much important as measuring that pressure precisely.
- The vacuum system must be flexible for upgrading and other future changes, also it needs to be designed with a reasonable cost for example by providing the machine with equipments which are available in the market not specially manufactured for SESAME.

7.4 General Layout

SESAME storage ring has 8 identical cells, see figure (7.1), each cell is divided into three sections: the straight section which is dedicated for the insertion devices, the RF cavities and the injection septum magnet, see figure (7.2). The second part is the arc, which contains the achromat section (the magnets region), this section contains the vacuum chamber through the dipoles, quadrupoles and sextupoles, see figure (7.3). The third part is the predipole vacuum chambers, see figure (7.4). Flanges connect the two parts to each other; besides, bellows with RF fingers are placed by the ends of each straight to absorb the thermal expansion and compression in the storage ring and to allow easy installation during assembly.

From vacuum point of view, SESAME storage ring will be divided into 7 sections, separated from each other by RF shielded gate valves, so each part will include two cells, i.e. four dipoles and three straights. The valves are situated in the short straight sections: two gate valves by the end of each RF straight, another gate valve located by the end of the injection straight, and one at SSS IV-2 straight, see figure (7.5).

Lumped absorbers provided with vacuum pumps located close to them, will absorb the unwanted synchrotron radiation. The layout of the storage ring is described in more details in chapter 5.

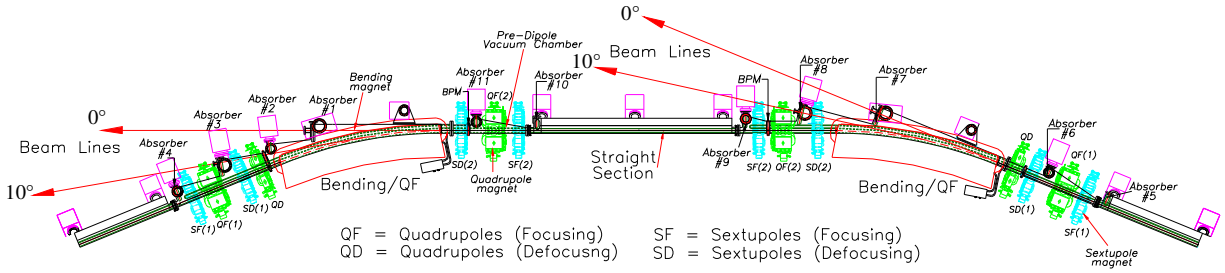

Figure 7.1 The unit cell of the storage ring.

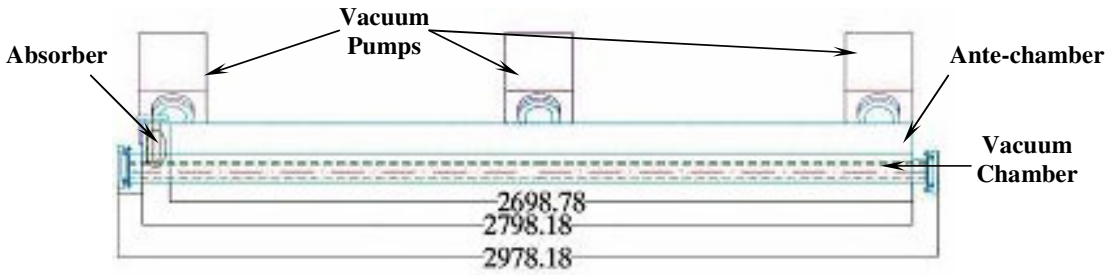

Figure 7.2: The straight section vacuum chamber.

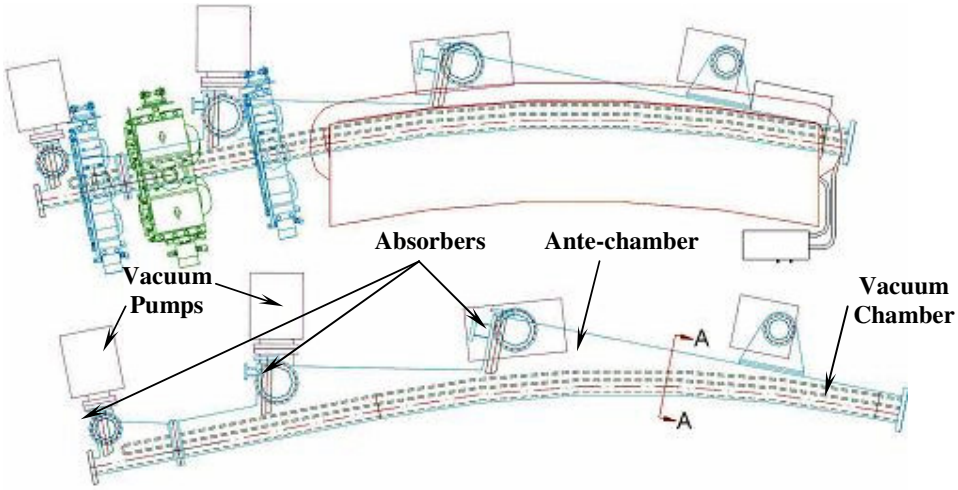

Figure 7.3: The achromat vacuum chamber.

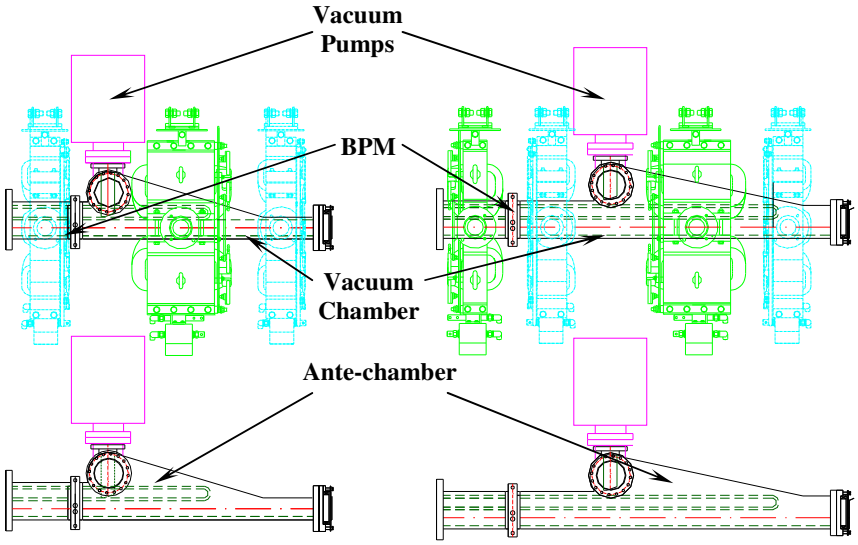

Figure 7.4: The pre-dipole vacuum chamber.

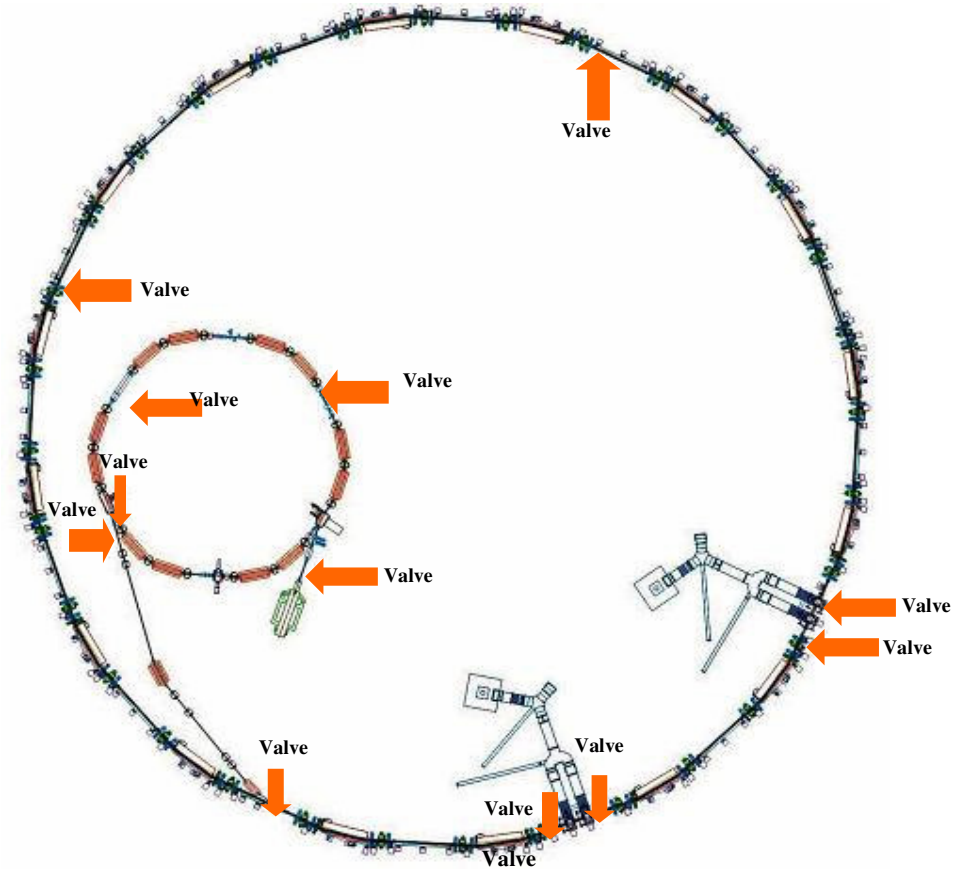

Figure 7.5: The locations of the valves distributed around the machine.

7.5 Materials for the Vacuum Chamber

In general, synchrotron light sources vacuum chambers are fabricated from the alloys of stainless steel, aluminium or copper. However copper is used inside the vessel as photon stopper or radiation absorbers, where high heat loads have to be dissipated.

The materials will be used for SESAME vacuum chamber must obey the vacuum and mechanical requirements, like the mechanical strength (stability and hardness), thermal conductivity, magnetic permeability, fabrication and joining…etc. [1], [2]

7.5.1 Proprieties

Unfortunately, there isn't one material that has all the required properties for synchrotron radiation sources' vacuum systems, so SESAME vacuum chamber will be fabricated from stainless steel (316LN) and OFHC copper will be used internally as synchrotron radiation absorber. The reasons behind this choice are described here.

7.5.1.1 Vacuum Performance

The vacuum performance of the material can be expressed by the photon desorption yield and its variation with the beam dose, and also with the "memory effect" of the material.

Figure (7.6) shows the measured values of photon desorption yield and its variation with the beam dose for stainless steel, aluminium and copper, respectively, for different gases.

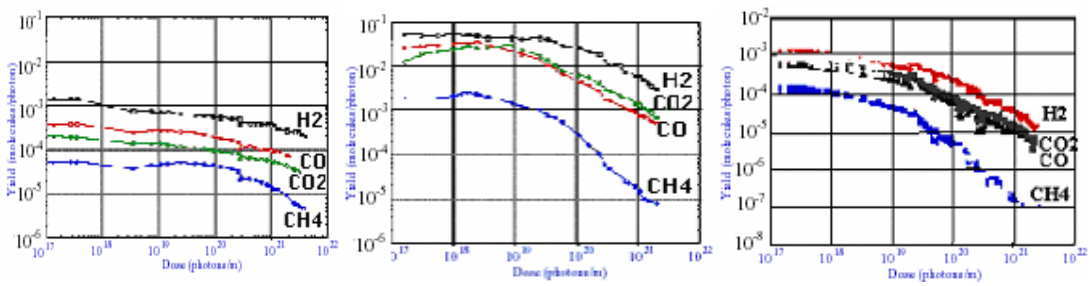

Stainless Steel **Aluminiu** **Copper**

Figure 7.6: Photon stimulated desorption yield variation with accumulated beam dose for stainless steel, aluminium and copper, respectively. [1]

It is clear from the curves that the main difference between the three is that aluminium has higher values of photon desorption yield than stainless steel and copper, but this is only true in the early stages of conditioning, and after that all have almost similar values for the desorption yield for the different gases.

Another important property required for the material to be used in the vacuum systems of the synchrotron sources is to have a good "memory effect", i.e. the desorption yield for scrubbed vacuum chamber need to have lower value than that for unscrubbed chamber after being vented, stainless steel and copper have a better memory effect than that of aluminium. [2].

7.5.1.2 Mechanical Properties

Aluminium has good properties such as: it is easy for manufacturing by extrusion especially for long beam tubes and complex chambers, also it is completely non magnetic. However aluminium has several disadvantages such as it has weak mechanical properties and it is difficult for joining.

In the other hand, copper (OFHC copper) has good thermal conductivity but its production process is more complicated and expensive in comparison to aluminium and stainless steel (if copper is used for vacuum vessels with an antechamber, the chambers need to be extruded separately from the antechamber and welded together afterwards). [3]

Stainless steel (316LN alloy is usually used for UHV applications for synchrotron light sources) has good mechanical strength; it is easy to weld and has high hardness also 316LN stainless steel is corrosion resistance alloy. Besides stainless steel has a low magnetic permeability, so it can be used within magnets. The thermal conductivity of stainless steel is very poor in comparison to copper, therefore to transport high heat loads (e.g. in absorbers) copper plates need to be used. Also stainless steel can be baked out up to (350ºC) to remove water and fired (up to 900ºC) to reduce H_2, such temperature must not be reached during bake out for aluminium. [3], [4]

There are another two arguments for choosing the material for the accelerator's vacuum chamber:

- One should use a material, which can be handled by the accelerator laboratory and there exist expertise to deal with them.
- The vacuum system should be build by the industry, so manufacturers should have good experience with the material to be used.

For all of these reasons, stainless steel was the best choice for SESAME vacuum chambers because of its suitable properties and OFHC copper should be used for the absorbers because of its good thermal conductivity.

7.5.2 Flanges and Gaskets

Knife-edge flanges (CF-Conflat® Flanges) are used in many synchrotron light facilities, as they are available commercially in many different standard diameters. However, the standard CF flange has a small cavity, which increase the total impedance and local heating. This is can be solved by using a metal seal which will close the gap, another way is by changing the design to have a smaller gap, this problem can also be solved by using flat seal flanges which have no gap between it and the gasket, this type of flanges has another advantage, these flanges have smaller size than CF flanges, as a result less material being used for their production and then have a lower cost [3].

For the small circular vacuum pipes, ordinary CF will be used, and for the elliptical vacuum chambers in SESAME, VAT® seals (which have flat sealing surfaces) can be requested, as they can take the shape of the vacuum chamber, experiments in some laboratories show their good performance. [5]

Silver coated copper gaskets will be used as they withstand the prebaking procedure before the final installation to the machine.

More detailed specifications for the flanges and the gaskets to be used for SESAME will be issued in the future.

7.6 Vacuum Chamber Design

The vacuum chamber can be divided into two sections; the achromat section which consists of the dipole vacuum chamber and sextupole and quadrupole magnets vacuum chamber, the second part is the straight section which is for the insertion devices, RF cavities and the injection septum. See figure (7.2) and (7.3).

The SLS approach have been adopted for SESAME vacuum chamber design, SESAME will be a full antechamber machine where synchrotron radiation will pass from the electron beam chamber through a slot to the antechamber towards the lumped absorbers located by the end of each antechamber section where large lumped pump is situated. [4], [6]

Concerning the introduction of the electrode of the BPM into the vacuum system, there are two methods have been adopted by the designers of the synchrotron light sources:

- Welding it directly to the BPM block.
- Using a separate flange to hold the electrodes, which are connected to the BPM block.

The BPM must be bolted rigidly to the magnet girders. To get rid of misreading of the BPM two options are available:

- The BPM electrode can be connected to the bellows to allow movement of the vacuum chambers.
- The movements of the vacuum chamber are detected by optical sensors and can be compensated for when reading the BPM. [4]

In order to avoid the extra cost of having a separate flange for the BPM the approach which will be adopted is to weld the BPM electrode directly to the BPM blocks and bolt it to the girders. The location of these BPM is shown in figure (7.7), one BPM will be located just before the dipole and one after the dipole magnet.

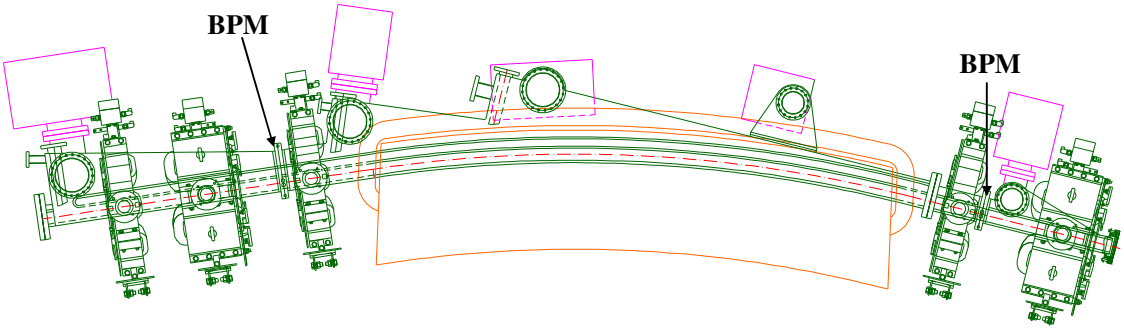

Figure 7.7: The locations of the beam position monitors.

Manufacturing should be done in such a way to eliminate trapped volumes (e.g. due to poor welding) to get better vacuum performance, since these volumes will increase the pump down time due to virtual leaks appearing. [7]

The detailed design of the vacuum chamber is represented in chapter 5.

7.7 Pumps Selection

7.7.1 Rough Pumping

The rough pumps are required to pump down the system from atmospheric pressure to below 10^{-6} mbar so that the UHV pumps can be started. The design should guarantee an efficient pumping and clean operation with the shortest possible time to reach the target pressure.

Mobile roughing stations are foreseen for SESAME, the main reason for this decision is to cut the cost of the roughing stations, as the number of the pumps required will be less in comparison to fixed stations, moreover, the use of mobile stations will save space in the storage ring, however, the use of mobile stations increases the cautions which need to be taken into consideration, especially the possibilities of contamination which are higher than if fixed stations being used, so control to the access of these pumps during storage must be done to reduce these chances.

The roughing station consists of fore-vacuum pump and a turbomolecular pump.

The fore-vacuum pump will pump down from atmospheric pressure to 10^{-2} mbar so the turbomolecular pump can be switched on, if drag turbomolecular pump being used then its operation can be started at higher pressure (1mbar), this will reduce the time required for pumping down, this pump will be adopted for the use in SESAME.

Diaphragm, piston or scroll pumps are possible types as baking pump for SESAME, but some characteristics will make one better than the others: time required to reach the target pressure, cost, the dimensions and the weight of the pump, noise level and if the pump has a built in isolating valve to prevent the backstreaming to the system in case of a power failure, and above all the cleanliness of the pump, which must be in the acceptable levels for the vacuum system specifications.

Magnetic bearing turbomolecular pump (maglev turbo) is the best choice in term of cleanliness for our application for pumping down at high vacuum pressure, however, the cost of such pumps is about twice that for ceramic bearings turbomolecular pumps (also ceramic bearing turbomlecular pumps are mounted in a restricted orientation).

In case the manufacturer guaranteed that the percentage of the hydrocarbons in the system is in the acceptable limit (typically < 1% of the total pressure) then it is suitable to use these pumps, many synchrotron light sources are using such pumps without any noticeable problem.

The main factors affecting the pumping down time are the distribution of the pumps around the unit cell, the size of the pump, the conductance along the beam tube and the volume to be evacuated.

Taking into consideration the conductance of the machine and as the conductance will limit the effective pumping speed of the pumps, it would be more sensible to use many pumps (and spread them around the cell) with a reasonable pumping speed rather than big pumps as this will reduce the pumping down time.

A pumping spout will be reserved near the first crotch absorber in the dipole to install the roughing station, it will be fitted with a 40mm aperture all metal valve. The station will also include a Pirani gauge, an inverted magnetron gauge and a let up valve.

The operation of the roughing stations will be manually. [8]

7.7.2 UHV Pumps

Capture pumps are the workhorse pumps required to achieve UHV in the vacuum systems for accelerators.

Ion pumps and titanium sublimation pumps are going to be used for SESAME; the reasons for this choice are described in this section.

The two types are clean pumps without any vibration (as they don't have any moving parts) also they do not need a valve to isolate them form the vacuum system. [9]

The ion pumps can be classified into three categories: the diode ion pump, the noble diode ion pump and the triode pump.

The diode ion pump is the standard sputter ion pump, which has a high pumping speed for all getter gases (and twice that of the triode ion pumps at 10^{-9} mbar) but this type of ion pumps has a very low pumping speed for noble gases (e.g. 2-5% of the pump pumping speed for Ar). Farther pumping, releases the previously buried noble gas molecules and as a result unstable pumping behaviour will be notice, this phenomena called (the instability of the noble gases).

The solution for this is either to use triode pumps or noble diode pumps; triode pumps will reduce the instability of the noble gases, the reason for this is the use of a negative voltage titanium grid instead of the ordinary cathodes, this approach will prevent the sputtering of the body or the anode as the energetic ions will not bombard the anode or the body of the pump, so the absorbed gases will stay bound on these surfaces.

Using noble diode pumps where the titanium cathode is replaced with tantalum cathode, will reduce the noble gases instability; the reason for this is that the instability depends on the reflection probability which is a function of the mass ratio of the ions species and the cathode material, so the instability will decrease as the atomic weight of Tantalum (181 AMU) is much higher than that of Ti (48 AMU). [10]

The replacement will not only reduce the instability but also will increase the pumping speed of the noble gases (about 20% of the pumping speed of air) but this will reduce the pumping speed of the active gases by 15% in comparison to the standard diode.

The titanium sublimation pump (TSP) is a very good solution for the need of high pumping speed at places of high outgassing rates. The pumping speed depends on the area being coated with titanium, so special care need to be taken when designing the TSP envelope in order to guarantee the highest possible surface area to be covered by the filament material.

For pumping down SESAME, diode ion pumps will be used and few noble diode ion pumps will be distributed around the ring to reduce the noble gases (at least one for each cell), also titanium sublimation pumps will be used either as a separate pump or combined with the ion pumps and are going to be used in places with high outgassing, like near the crotch absorbers.

Concerning the operation range of the ion pumps, all the pumps must be able to operate at pressures from $5 \cdot 10^{-3}$ mbar down to $1 \cdot 10^{-10}$ mbar, but operation at pressures over 10^{-5} mbar need to be prevented, as this will reduce the life time of the pump. The titanium sublimation pumps must be conditioned and fired carefully taking into consideration that the pressure should not increase over $1 \cdot 10^{-7}$ mbar during the firing process, also ramping the power need to be in steps, so manual conditioning for the TSP is required. At 10^{-9} mbar pressure range, the TSP can be fired once every few days only.

The pumping ports of the pumps are of circular shape directly connected to the antechamber; as a result, there isn't any need for the use of RF screen to separate the pump from the system.

A recent approach in many synchrotron light sources is to bake out the ion pumps (also the TSP), so heaters need to be installed inside the body of the pump, this approach will not only decrease the conditioning time of the machine, but also it will be an advantage in case NEG ribbons being fitted to the pump (to increase the pumping speed) as this will activate the NEG. [11].

The power supplies for the ion pumps must be able to display the current, the voltage and the pressure as such information are very useful to estimate the pressure profile along the achromat.

The control units of the pumps must provide at least one relay set point for each HV channel, more detailed specifications for the ion pumps and the TSP control units and power supply units will be issued in the future. [12]

Newly designed machines adopted the NEG coating techniques in the design of the vacuum system like in Soliel and Diamond (also existing machines are replacing their old vacuum chambers with new coated like ESRF). NEG coating is a very good solution for systems having conductance limitations, but NEG coating required activation by heating, for non in-situ baked systems the activation of the NEG will be a problem. As for SESAME, this technology could be adopted for the small gap insertion devices as this will solve the limitation of the conductance, or installing NEG strips in the antechamber (with electrical feed through for activation) will provide a very good vacuum at these places.

7.8 Vacuum Instrumentation

The measurement of vacuum is as much important as providing the required vacuum, the total and partial pressure must be measured correctly. General specifications for both the total pressure gauges and the partial pressure gauges with the locations of the gauge heads throughout the facility are described here.

7.8.1 Total Pressure Gauges

As the total average dynamic pressure needs to be around 1.10^{-9} mbar, then the gauges required for SESAME should be able to read a pressure of $1 \cdot 10^{-10}$ mbar which is the pressure required before the beam being injected. The injector pressure measurement system requires a reliable reading down to $1 \cdot 10^{-9}$ mbar.

Unfortunately, it is not possible to cover the whole pressure range with a single gauge; a gauge is required to cover the low vacuum range (from atm. pressure to 10^{-3} mbar) such a gauge will be useful to provide reading during pumping down the system and during vacuum failure. A second gauge is required for UHV readings (for ranges of 10^{-3}-10^{-10} mbar).

For low vacuum range, since the reading is just required to give an indication of the general situation of the vacuum system, so a gauge such as Pirani gauge is a good choice, as it covers the range from atm. to 10^{-3} mbar. The gauge should be bakeable up to 250ºC, and the control unit should provide two relay set points interface over the measured pressure range.

For the UHV range, two types of gauges are in common use on the accelerators around the world: cold cathode gauges and hot cathode gauges.

The hot cathode gauge needs a third gauge to cover readings between 10^{-3} and $5x10^{-4}$ mbar, also the hot cathode gauge has a filament which could burn in case of vacuum failure, but this is not the case with the cold cathode gauges, also it has a high outgassing in comparison with the cold cathode gauge.

For the cold cathode gauges, penning discharge cold cathode gauge does not cover pressure values below 10^{-9} mbar, while inverted magnetron discharge cold cathode gauge covers pressure ranges from 10^{-3} down to 10^{-11} mbar.

For all of the previous reasons, inverted magnetron cold cathode gauge (IMG) seems the best choice for SESAME, the gauge head should be bakeable to 250ºC, and each gauge control unit should be able to operate at least two inverted magnetron and two Pirani gauges or 3 IMG and a Pirani.

Each part of the accelerator must be covered by a pressure gauge. In general, each vacuum section (area between two gate valves) should contain two pairs of total pressure gauges. A pair of total pressure gauge is also required for the Microtron, RF cavities, injection straight section, the transfer lines, the roughing stations, all should have at least one pair of total pressure gauges.

The location of the gauge need to be selected in a way which guarantees that there isn't any exposure to mechanical or magnetic noise and as far as possible from radiation which could destroy the electronics of the gauges. For SESAME the gauges are going to be installed near the first or the second crotch absorbers, a remark could be pointed out that the gauges will be close to the lumped pump which have a high pumping speed, so the gauges may not give the right reading of the pressure. The reason for the selection of this location that even that the gauge is close to high pumping speed but it is also close to the places with high outgassing, and in order to identify the pressure in the rest of the cell and to get a complete pressure profile, the voltage and current of the ion pumps will be used to identify the pressure, and this was the main reason of using only two total pressure gauges per cell. [13], [14]

The control units of the gauges should be connected to the EPS (Equipment Protection System), which is in its turn need to be connected EPICS.

7.8.2 Partial Pressure Gauges

It is important for UHV applications to know the composition of the residual gases within the system. Quadrupole mass spectrometer used as Residual Gas Analyser (RGA) measures the partial pressure of the gases in the system will be used for SESAME.

At least one RGA is required for each part of the accelerator (i.e. one RGA per vacuum cell); also at least one is required for the Microtron, the injector vacuum system, the injection straight section, the RF cavity and the ID straight section. In order to cover the rest of the machine it is recommended to have blank flanges separated from the machine by all metal valves, where residual gas analysers can be installed when there is a need for that. Such fanges are going to be useful for other vacuum requirements and applications.

The heads should be bakeable to 250ºC, and the RGA should cover a range between 0-200 AMU, however, residual gas analysers which cover up to 100AMU only can be used as they are cheaper than those cover up to 200AMU (also it is unusual to get gases in the system with masses higher than 100AMU), but (and just be to in the safe side) at least one must cover to 200AMU and it could be used as a portable RGA.

More detailed specifications for the RGA heads and control units will be issued in the future.

Control units of all the gauges and the other vacuum equipments need to be provided with all necessary cables, interlocks, front panels… etc, and they should have the ability to influence the main control system. [13]

Figure (7.8) shows a vacuum flow diagram for one of SESAME cells. This diagram shows the locations of the pumps, gauges and the valves.

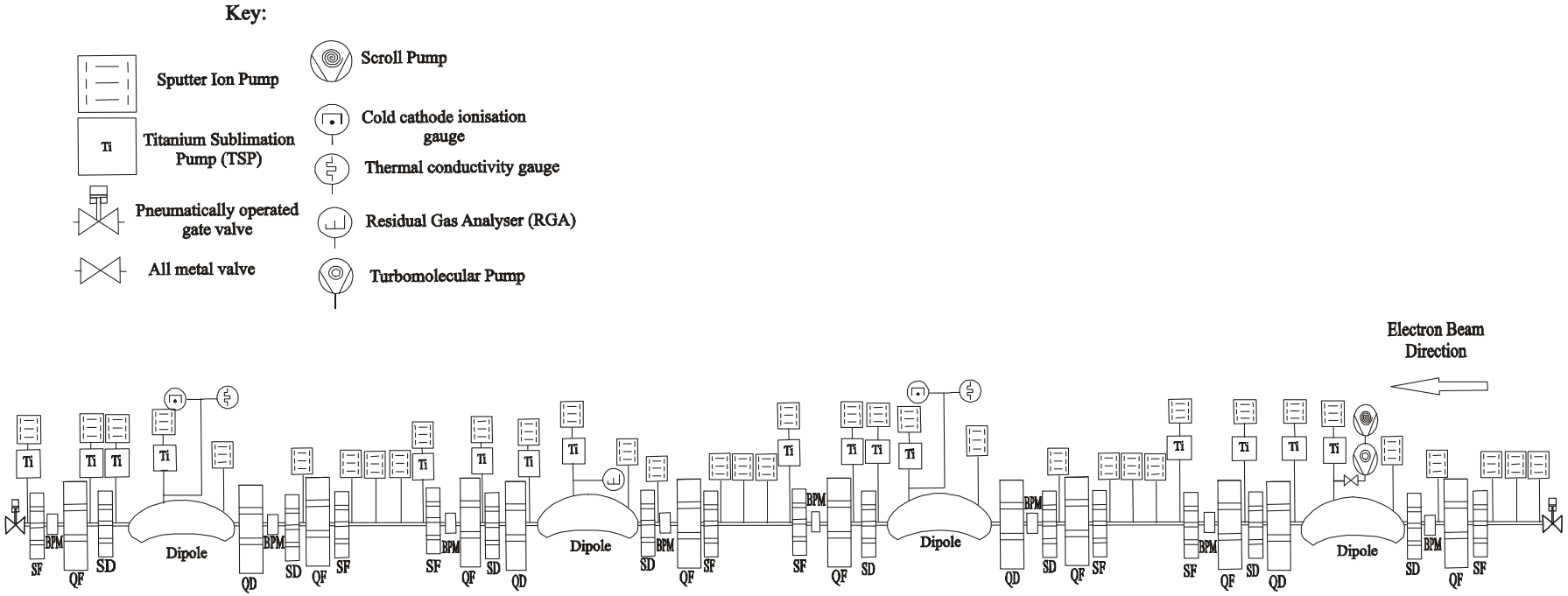

Figure 7.8: SESAME vacuum flow diagram (gauges, pumps and valves types and locations)

7.9 Cleaning, Bakeout and Infrastructure.

The decision was made not to bakeout in-situ in order to cut the cost of the heaters, insulation and most importantly the size of the magnets will be smaller, so cheaper magnets will be used. A careful and a good preparation of the vacuum components before installation is required in order to reach the target pressure.

All components need to be cleaned properly. Cleaning procedures must guarantee that all components will be suitable for UHV. Cleaning will reduce the evolution of the gases from the surface; the source of these gases can be oils, greases, fluxes, fingerprints…etc. Cleaning should be suitable for the material type and should not leave any deposits behind. [15]

Many factors will decide the cleaning procedure; the target pressure, the material to be cleaned, safety regulations, cost…etc.

The cleaning procedure has been described for many materials for UHV application in many literatures, for SESAME and as stainless steel is the material of the vacuum chamber, then the following procedure is proposed in reference [15] to reach the required pressure:

1. Wash with a high pressure hot water (80ºC) mixed with mild alkaline detergent.
2. Wash with hot water only to remove the detergent.
3. Drying the component with a blower of dry clean hot air.
4. Immerse completely in ultrasonic bath of clean hot solvent for 15 minute.
5. Leave the component in the vapour (the pure state) of the solvent for 15 minute.
6. Wash with demineralised pressurised hot water.
7. Immerse in a hot alkaline degreaser with ultrasonic agitation for 5 minutes.
8. Wash with demineralised pressurised hot water.
9. Dry with clean dry air.

After the cleaning, the components need to be baked under vacuum to 250ºC for at least 24 hours to desorb water molecules.

It is very important to mention that care needs to be taken during the cleaning, as some chemicals are toxic.

Such a procedure is essential for all components facing vacuum, however, the cost is an important issue for SESAME, (for large parts (e.g. the dipole vacuum chamber) this will require large cleaning tanks and large ovens, which means high cost). The solution for this is to follow the cleaning procedure in SESAME facility for small parts, but for large contaminated parts need cleaning they need to be sent for cleaning and bakeout in specialised companies for cleaning, and have a spear parts of these vacuum chambers which have been cleaned, baked and stored under vacuum for the use when the contaminated large parts are in cleaning. Another approach being followed in some laboratories (e.g. SLS) is to depend more on long bakeout periods (which required large ovens or oven modules) without having a large cleaning facility.

The machine need to be supplied with dry nitrogen for use if venting of the machine is required, and the specification of the cleanliness and the humidity level of the nitrogen need to be investigated carefully, as this have a big impact in the outgassing rates of the different parts.

Compressed air is also required for the successful operation of the gate valves, the compressed air should be clean and at a pressure of 8bar. Helium is also required for leak chasing purposes. [16], [12]

A vacuum laboratory is required in the SESAME facility; there must be (in addition to the cleaning facility) a place for assembling and handling and clean rooms, also a storage is required.

It would be important to have a mechanical workshop in the early stages of the operation, as such a workshop with well-trained technicians will provide the facility with maintenance and the required components, and that will reduce the running cost of the machine.

7.10 Assembly

The assembly procedure is an important issue from vacuum point of view, the pumps and the vacuum chamber must be supplied stored under vacuum, and when they are assembled to the machine, they should not be exposed to atmosphere except after let up by dry nitrogen and after that they should not exposed to atmospheric air for long time, as the longer they exposed to air, the longer it will take to be pumped down. The assembly need to be done under a tent filled with nitrogen to guarantee the shortest possible pumping time.

7.11 Pressure Profile Calculations

In order to achieve a good beam lifetime in the storage ring; the average dynamic pressure inside the vacuum chamber must be as small as possible. The average pressure is defined by the location of the pumps, the pumping speed, the outgassing of the vacuum chamber and the cross section of the vacuum chamber and profile and other factors.

For the optimisation of the location of the pumps and their pumping speed; the pressure profile calculations have to be performed.

The evaluation of the pressure profile can be done in several ways; one of the possible ways is by using Monte-Carlo Simulation, to apply the simulation, the full detailed geometry of the vacuum chamber need to be designed, unfortunately the complete detailed design of SESAME is not finalised yet, so the estimation of the pressure profile will be done analytically by using a program written in MathCAD by Dr. Oleg Malyshev from SRS at CCLRC Daresbury Laboratory-UK.

The calculations will be performed based on the gas dynamic balance equation inside a vacuum chamber, equation (7.1), [17]

$$V\frac{dn}{dt} = q - cn + u\frac{d^2n}{dL^2} \tag{7.1}$$

Where:

- V is the vacuum chamber volume,
- n is the gas density (density number),
- u is the specific vacuum chamber molecular gas flow conductance per unit axial length.
- L is the longitudinal axis of the vacuum chamber,
- c is the distributed pumping speed,
- q the gas desorption flux from both thermal desorption and photo stimulated desorption, given by equation (7.2).

$$q = \eta_t F + \eta\gamma\Gamma \tag{7.2}$$

Where:

- F is the surface area exposed to vacuum.
- Γ is the photon flux.
- η_t , $\eta\gamma$ are the thermal and photo stimulation desorption yields.

A detailed discussion along with the solution of the gas dynamic balance equation for the gas volume density (n) is presented in reference [17].

7.11.1 Gas Load Generation and Desorption Processes

The outgassing process controls the gas composition and the ultimate pressure achieved in the system.

In the storage ring, the synchrotron radiation impinging the vacuum chamber walls and the absorbers producing a strong outgassing and thus increasing the dynamic pressure.

There is two discrete desorption processes: the thermal desorption and the photon stimulated desorption.

7.11.1.1 Thermal Desorption

All the surfaces facing vacuum desorbs gas into the system; the thermal desorption will define the base pressure of the system without the electron beam.

The thermal desorption (q_{th}) can be evaluated by multiplying the total surface area (around $1.2 \cdot 10^6$ cm^2) by the thermal outgassing rate of the material, ($\eta_t = 10^{-12}$-10^{-11} mbar.L/sec.cm^2, the value depends on the material, preparation techniques, cleaning.. etc). The areas need to be included in the calculations are all the areas facing vacuum, i.e. the vacuum chamber, the antechamber, the pumping ports and the front ends (up to the first valve of the beam line) as a result the expected thermal desorption load to be $1.15 \cdot 10^{-5}$ mbar·L/s.

It is significant to mention that in order to reduce the thermal outgassing out from the surfaces, it is essential to bakeout the different components up to 250ºC for at least 24 hours before installation, in addition, it is possible to decrease the water contents on the surface by using dry nitrogen when letting up the chamber in case of venting of the system, as nitrogen desorbes much more easily than other gases, however, a special attention need to be taken to the quality and the specifications of the nitrogen will be used for let up. [18]

7.11.1.2 Photon Stimulated Desorption (PSD)

Photon stimulated desorption occurs when photons interact with the vacuum chamber surface producing photoelectrons which in its turn produce the desorption of the molecules by the electron stimulated desorption. For systems where synchrotron radiation hits only in lumped absorbers not the vacuum chamber walls (which is the case with SESAME), the amount of photoelectrons is reduced and hence the desorption of molecules is decreased. [6]

The quantity in interest is the photon induced gas desorption yield (η) which is the number of desorbed gas molecules per induced photon, which decreases with the photon dose proportionally, $D^{-\alpha}$, where D is the dose and the coefficient α varies from 2/3 to 1. For the calculations, α will be used as 2/3 as this value will give higher PSD and for not in-situ baked vacuum chamber, as this will be the case for SESAME.

Figure (7.9) shows the (experimental) results of the variation of η with the beam dose (photon flux by the time) for CO (mass 28) for unbaked in-situ and in-situ baked vacuum chamber.

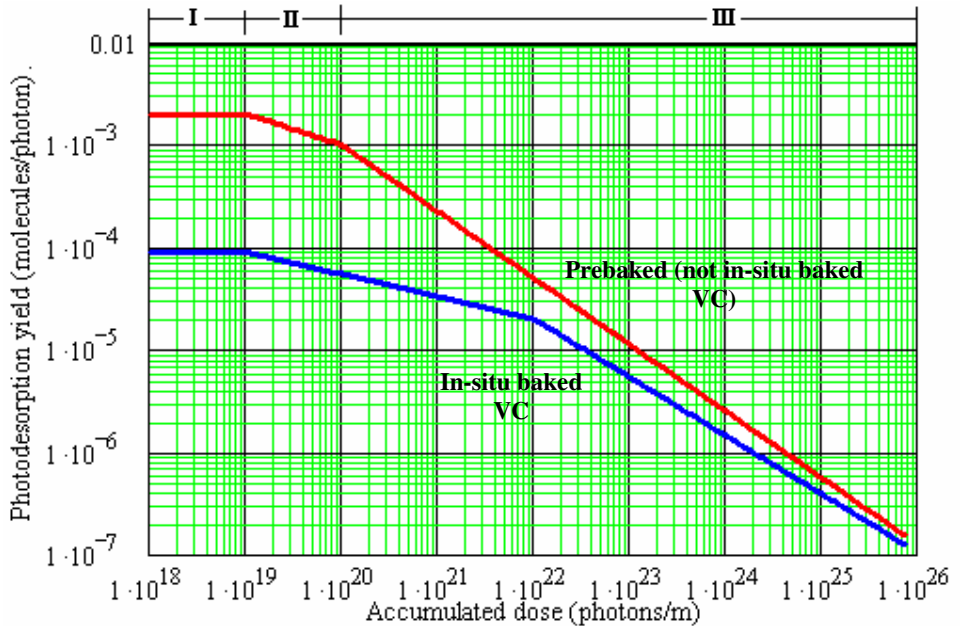

Figure 7.9: Photon stimulated desorption yield for CO (AMU 28) for in-situ baked and for prebaked vacuum chamber.

For the calculation purposes the pre-baked (not in-situ) curve has been divided into 3 regions, based on the slop of the curve, equation (7.3) shows the value of η based on the dose value.

$$\eta = \begin{cases} 0.002 & D \le 10^{19} \quad \text{I} \\ 0.002\left(\frac{10^{19}}{D}\right)^{0.3} & 10^{19} < D \le 10^{20} \quad \text{II} \\ 2\times 10^{-3}\left(\frac{10^{20}}{D}\right)^{0.65} & \text{otherwise} \quad \text{III} \end{cases} \tag{7.3}$$

7.11.2 Photon Flux from the Dipole

For the calculation of the photon stimulated desorption, the photon flux from the dipole need to be evaluated.

The radiation from the dipoles will find its way into 3 possible places: 1) to the crotch absorbers 2) to the beam line front ends 3) It irradiates the walls of the vacuum chamber, see figure (7.10). SESAME is designed in a way that almost all unused synchrotron radiation to be absorbed by lumped absorbers installed after each bending magnet. Table (7.2) shows the estimated amount of mrads of the radiation fan each absorber will get from the dipoles. The amount of mrads which will irradiate the walls of the vacuum chamber from one cell (two dipole) is 14mrad. Figure (7.11) shows the distribution of the absorbers along one cell of SESAME.

In addition it was assumed (for the calculations) that 20% of the radiation would hit the top and bottom of vacuum chamber walls.

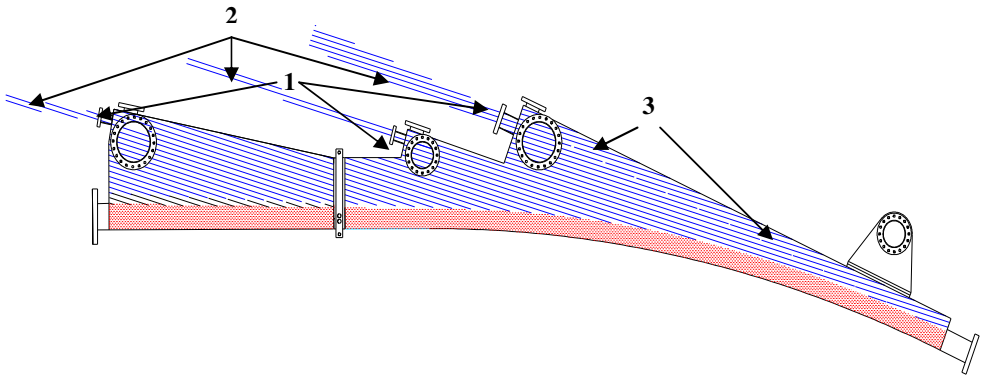

Figure 7.10: The radiation will hit: 1- the absorber, 2- the front ends, 3- the vacuum chamber walls.

Table 7.2: The amount of radiation to be reached by each absorber.

Absorber #	mrad
1	109.8
2	58
3	118
4	89
5	8.3
6	3.2
7	137
8	153
9	76
10	17
11	1.6

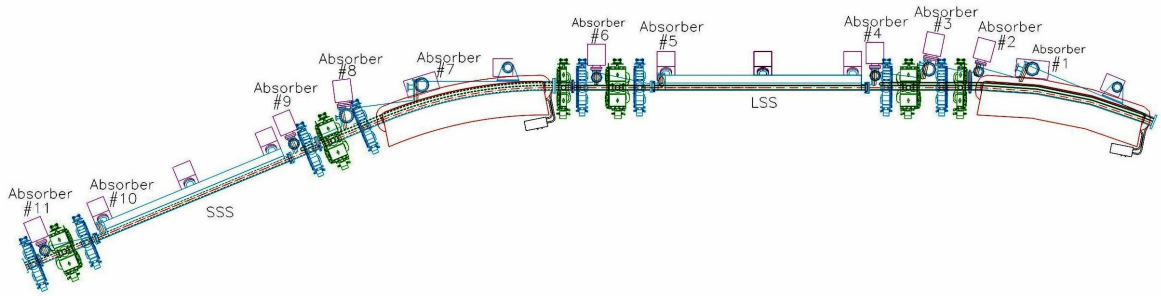

Figure 7.11: The distribution of the absorbers along one cell of SESAME.

Equation (7.4) has been used to evaluate the total photon flux (photons/sec) from the dipoles.[1]

$$\Gamma_{tot} = 8 \cdot 10^{17} \cdot E \cdot I \qquad (7.4)$$

With beam energy of 2.5GeV and 400mA beam current, the value of Γ_{tot} is $8.042 \cdot 10^{20}$ photons/sec. So the contribution from each dipole is $5.027 \cdot 10^{19}$ photons/ sec. dipole.

Equation (7.5) shows the photon flux per metre length of the vacuum chamber from the end of the dipole (photons/m.s).

$$\Gamma(L) = \Gamma_{rad} \cdot \frac{\left(R_d + a\right)\sqrt{L^2 + 2R_d.a + a^2} - LR_d}{\left[\left(R_d + a\right)^2 + L^2\right]\sqrt{L^2 + 2.R_d.a + a^2}} \qquad (7.5)$$

Where:

$\Gamma(L)$ is the photon flux (photons/m.s) at L length from the dipole.

a is the long radius of the elliptical vacuum chamber.

Γ_{rad} is the angular photon flux (photon/rad.s), $\Gamma_{rad}=1.28\cdot10^{20}.E.I$

R_d is the bending radius.

The description of the different parameters being used in this equation is shown in figure (7.12).

Figure (7.13) shows the photon flux distribution along the dipole ($2.174\cdot10^{19}$ photon/s.m) and along the straight section, the minimum value for the photon flux is just before the following bending magnet with a value of ($1.49\cdot10^{17}$ photon/s.m). This figure shows the amount of radiation that may hit the vacuum chamber in case there is not any antechamber there.

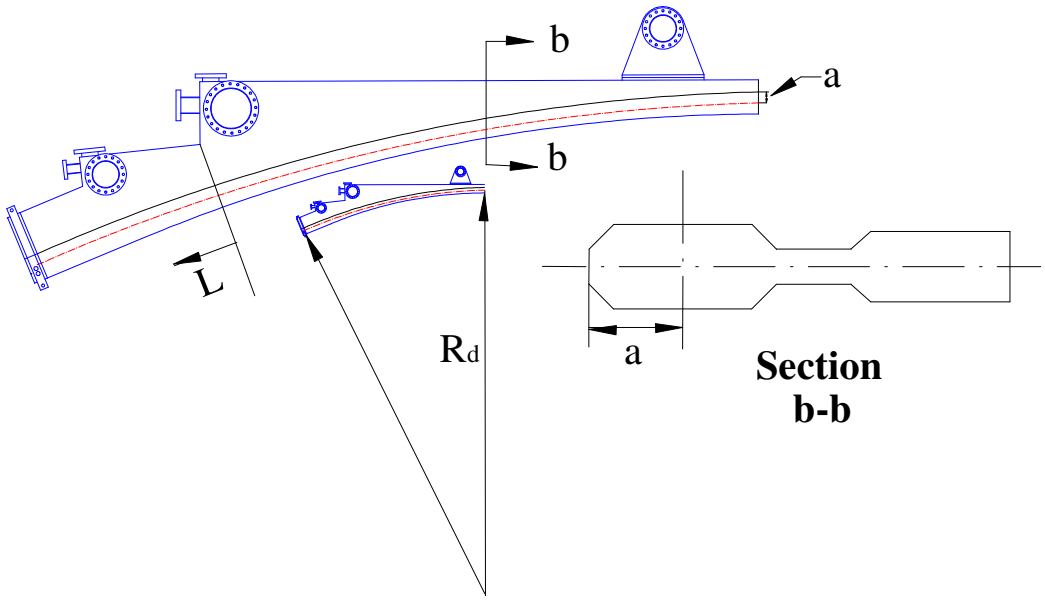

Figure 7.12: Description of the parameters in equation (7.5).

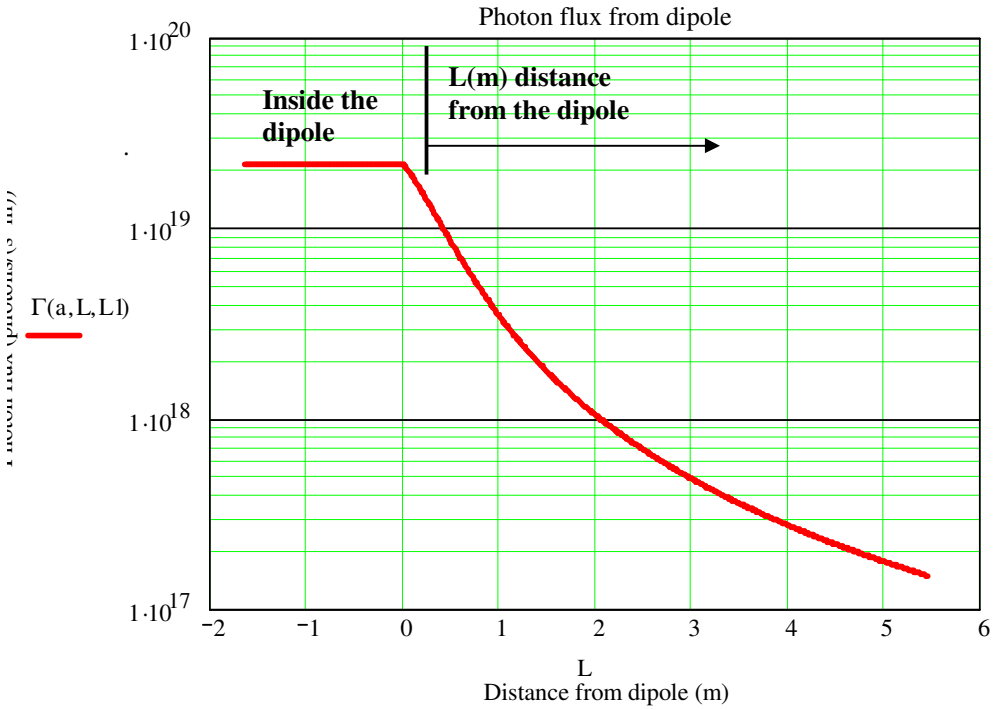

Figure 7.13: The photon flux from the dipole per metre distance from the bending magnet.

7.11.3 Photon Stimulated Desorption Yield for SESAME (PSD)

As the photon stimulated desorption yield varies with the dose, and as the dose varies with photon flux which is variable with the distance from the dipole, then the value of the photon stimulated desorption yield will also vary with the distance. Figure (7.14) shows the photon stimulated desorption yield variation with the distance from the dipole for different conditioning time (dose rate). As it is shown in the figure, the PSD yield is maximum during the first stages of the conditioning process (around $4 \cdot 10^{-3}$ molecules/photon during the first operation), and as the beam cleaning process for the vacuum chamber increases (at higher doses) the value will decrease until a value in the range of 10^{-5} molecules/photon being achieved after 100Ah beam dose, and this will decrease more and more for higher doses.

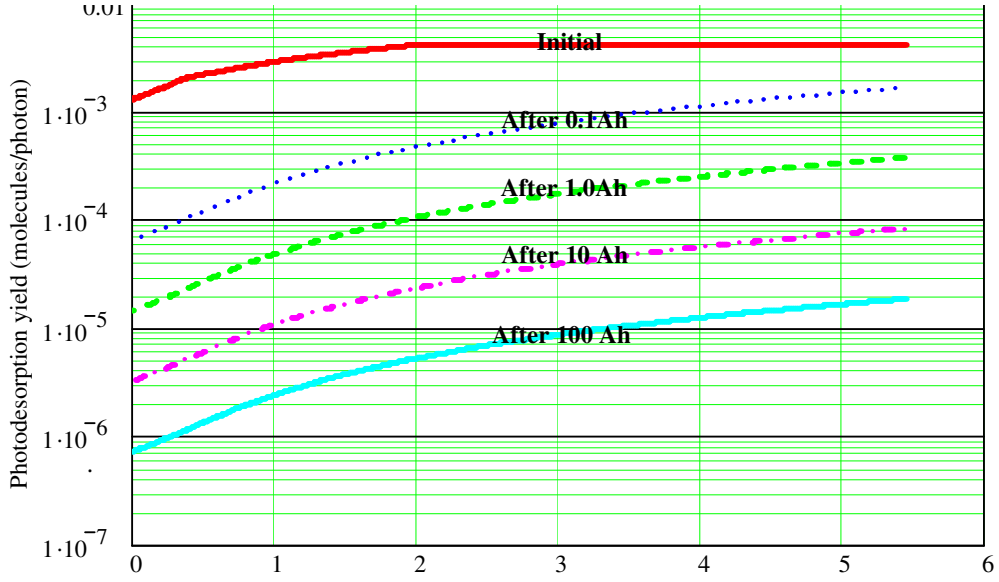

Figure 7.14: Photon stimulated desorption yield variation with distance from the bending magnets for different beam doses.

7.11.4 Desorption Flux

The desorption flux (molecules/s.m) can be achieved simply by multiplying the photon stimulated desorption yield by the photon flux which both are function of the distance from the dipole. Hence, the desorption flux will be a function of distance and also the dose. The desorption flux variation with the distance is shown in figure (7.15), the curves are the multiplication of the curve in figure (7.13) and the curves in figure (7.14).

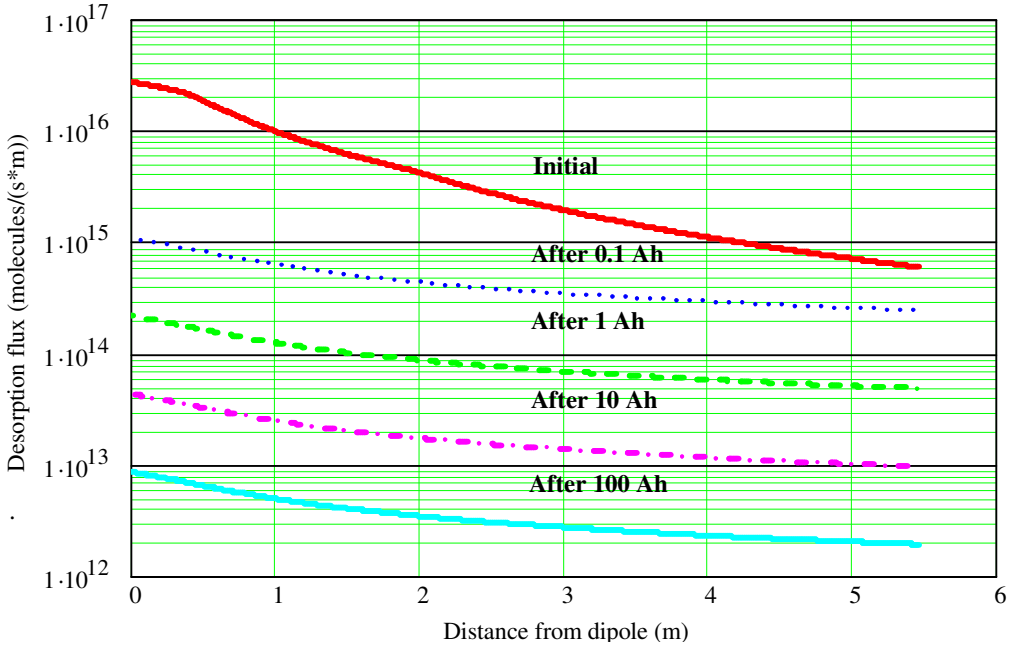

Figure 7.15: The desorption flux variation with the distance from the dipole for different beam dose.

7.11.5 The Achromat Pressure Profile

The following step in the calculations is to add the geometry of the vacuum chamber in order to evaluate the pressure profile along the storage ring cell, from both the thermal desorption which will give the base pressure "without beam" and the photon stimulated desorption which will give the dynamic pressure "with the beam".

To evaluate the pressure profile, the vacuum chamber achromat has been divided into parts, each part is defined by its length, if a pump is connected to it or not, and the type and amount of pumping. Also it will be defined by the amount of photon flux it will get, and if it has an antechamber or not.

Table (7.3) shows part of the databases for the vacuum chamber of SESAME. l is the length of the section, L is the accumulated length from the beginning of the achromat, X is half the horizontal aperture of the vacuum chamber, and Y is half the vertical aperture of the vacuum chamber, pumping will give the amount of pumping speed of the pumps for each section, and photons column describes the amount of radiation each section will get.

Table 7.3: Part of the vacuum components list of the SESAME achromat for the pressure profile calculations, the vacuum chamber is divided into sections for the calculation purposes.

Achromat vacuum chamber elements							
l (mm)	**L (mm)**	**X (m)**	**Y (m)**	**Pumping**	**Photons**	**Antechamber (m)**	**Element**
100	100	0.035	0.015	1	1	0.2	Pump
1290	1390	0.035	0.015	0	1	0.2	VC
100	1490	0.035	0.015	1	5	0.2	Absorber + pump
132	1622	0.035	0.015	0	1	0.0317	VC
662	2284	0.035	0.015	0	1	0.137	VC
100	2384	0.035	0.015	1	6	0.165	Absorber + pump
578	2962	0.035	0.015	0	1	0.04	VC
437	3399	0.035	0.015	0	30	0.065	Dipole VC
300	3699	0.035	0.015	2	30	0.09	Pump
926	4625	0.035	0.015	0	30	0.233	Dipole VC
150	4775	0.035	0.015	3	7	0.3	Absorber + pump
650	5425	0.035	0.015	0	30	0.196	Dipole VC
284	5709	0.035	0.015	0	1	0.247	VC
150	5859	0.035	0.015	3	8	0.346	Absorber + pump
458	6317	0.035	0.015	0	1	0.105	VC
232	6549	0.035	0.015	0	1	0.173	VC
100	6649	0.035	0.015	4	9	0.18	Absorber + pump
143	6792	0.035	0.015	0	1	0	VC
74	6866	0.035	0.015	0	1	0.2	VC
100	6966	0.035	0.015	1	1	0.2	Pump
1117	8083	0.035	0.015	0	1	0.2	VC
100	8183	0.035	0.015	1	1	0.2	Pump
1247	9430	0.035	0.015	0	1	0.2	VC
100	9530	0.035	0.015	1	10	0.2	Absorber + pump
634	10164	0.035	0.015	0	1	0.122	VC
100	10264	0.035	0.015	1	11	0.13	Absorber + pump
356	10620	0.035	0.015	0	1	0.04	VC
437	11057	0.035	0.015	0	30	0.04	Dipole VC
300	11357	0.035	0.015	2	30	0.09	Pump

7.11.5.1 Pumps Pumping Speed and the Average Dynamic Pressure

With these inputs and with nominal pumping speed for the pumps as follow (see figure (7.16):

- Pumps indicated as 1 and 2 in the above table are ion pumps with a nominal pumping speed of 150L/s.
- Pumps indicated as 3 in the above table are ion pumps combined with TSP with a nominal pumping speed for ion pumps of 500L/s, the expected total pumping speed is 700L/s.
- Pumps indicated as 4 in the above table are ion pumps combined with TSP with a nominal pumping speed for ion pumps of 300L/s, the expected total pumping speed is 500L/s.

The total nominal pumping speed of the ion pumps for the storage ring is around 32,000 L/s, in comparison with similar machines (energy and current) SESAME laid between SLS (38,000 L/s) and the CLS (30,000 L/s).

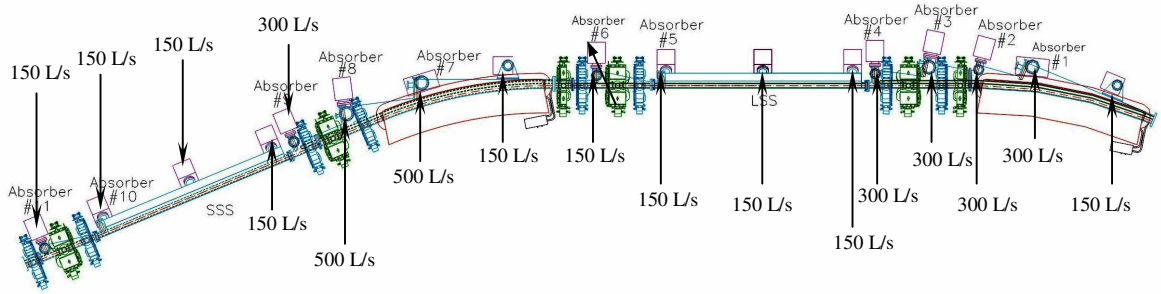

Figure 7.16: the pumping speed of the ion pumps around SESAME unit cell.

From the above inputs, the pressure profile was calculated for different situations, in case the operation of SESAME from the beginning was with 2.5GeV beam energy and with the maximum beam current 400mA, then the expected average dynamic pressure will be over the acceptable level (the range 1.10^{-9} mbar). Figure (7.17) shows the base pressure profile (due to thermal desorption / without SR beam) and the dynamic pressure (due to both the thermal and the photo stimulated desorption / with SR beam) at 200Ah and beam current of 400mA, and an energy of 2.5GeV, the average base pressure was calculated with a value of $P_{av,T} = 4.79 \cdot 10^{-10}$ mbar, the average pressure due to photon stimulated desorption is $P_{av,PSD} = 1.98 \cdot 10^{-9}$ and the average total dynamic pressure is: $P_{av} = 2.46 \cdot 10^{-9}$ mbar.

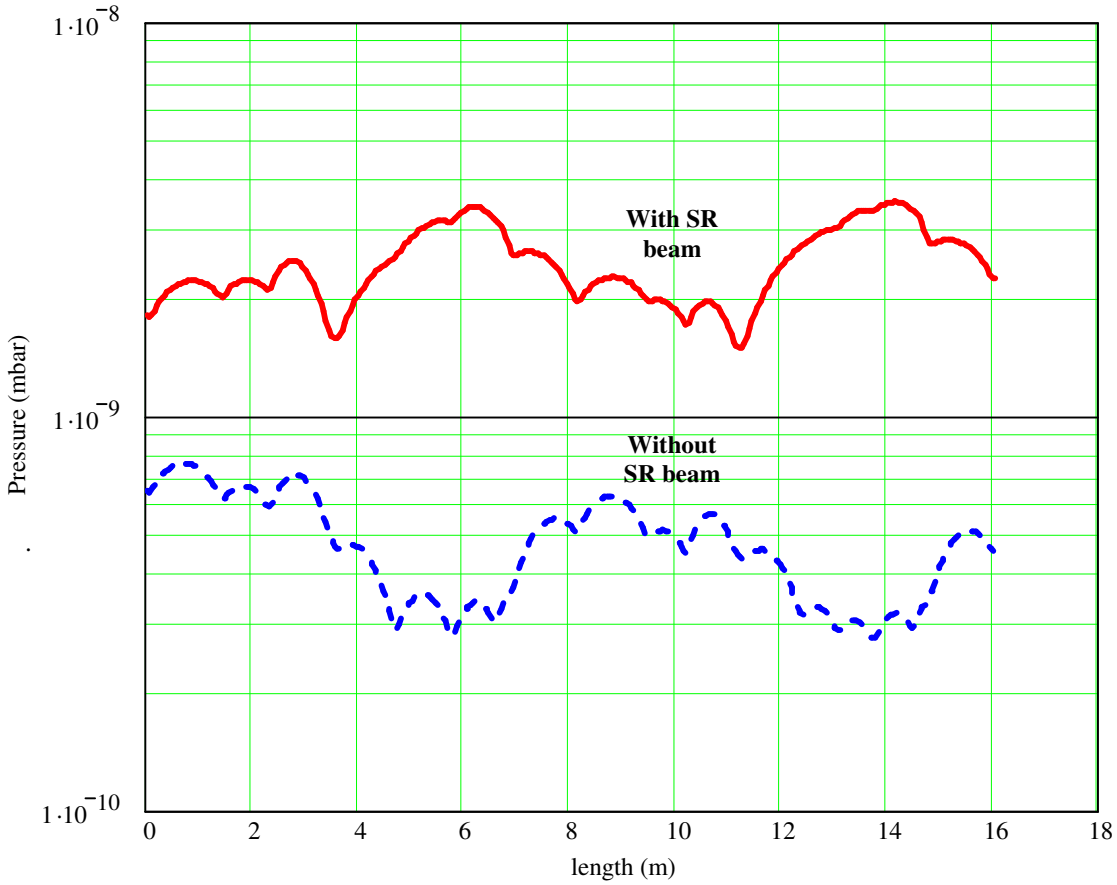

Figure 7.17: Pressure profile for 1/8 of the storage ring, $P_{av,T} = 4.787 \cdot 10^{-10}$ mbar, $P_{av,PSD} = 1.98 \cdot 10^{-9}$ mbar, $P_{av} = 2.46 \cdot 10^{-9}$ mbar, at 200Ah, 400mA.

The behaviour of the pressure profile curve is as it is expected; the highs and lows of the curve represent places without pumps and/or with high outgassing and places with pumps, respectively. The highest values of the pressure were in places with high outgassing rates; i.e. in the dipoles and close to the crotch absorbers, the maximum value for the pressure at these areas is: $P_{av}=3.5 \cdot 10^{-9}$ mbar, and the lowest value was just before the following dipole (in the pre-dipole area) as this location, is the area which has the lowest outgassing rate, the average total pressure in the pre-dipole is $P_{av}=1.8 \cdot 10^{-9}$ mbar.

In addition, and as the figure shows, at the dipole vacuum chamber, the average base pressure is quit low simply because of the high conductance at these places due to the wide antechamber so it is easy to pump down there without losing a lot from the pumps pumping speed, on the other hand, the pressure due to PSD is high there, simply due to the high outgassing rates.

7.11.5.2 Changes in the Pumps Pumping Speed and the Average Dynamic Pressure Achieved.

Some changes with the pumping speed could help in achieving better vacuum, for example (and under the same conditions described in the previous section) increasing the pumping speed of the pump close to the absorber No. 1 and 3 into 500L/s (from the ion pumps, i.e. pumping speed similar to absorber No. 7 and 8 will reduce the pressure with a value for the

dynamic average pressure of $P_{av}=2.33\cdot10^{-9}$ mbar. However, the cost of such pumps is high, so keeping the pumping speed of the ion pumps as mentioned in section 7.11.5.1 is proposed with the need of additional pumping from TSP will be enough. The average dynamic pressure will be reduced due to beam cleaning effect of the vacuum chamber as discussed in the following section.

7.11.5.3 Average Dynamic Pressure of the Achromat During Commissioning and Operation of the Machine.

SESAME will not run under the optimal conditions from day one or even after a while from its operation: in the beginning SESAME will operate with two RF cavities, so SESAME will run at 2GeV and with current of 200-250mA. Figure (7.18) shows the pressure profile under these conditions I=200mA at 200Ah dose and at energy of 2.0GeV, the expected average dynamic pressure is $1.42\cdot10^{-9}$ mbar.

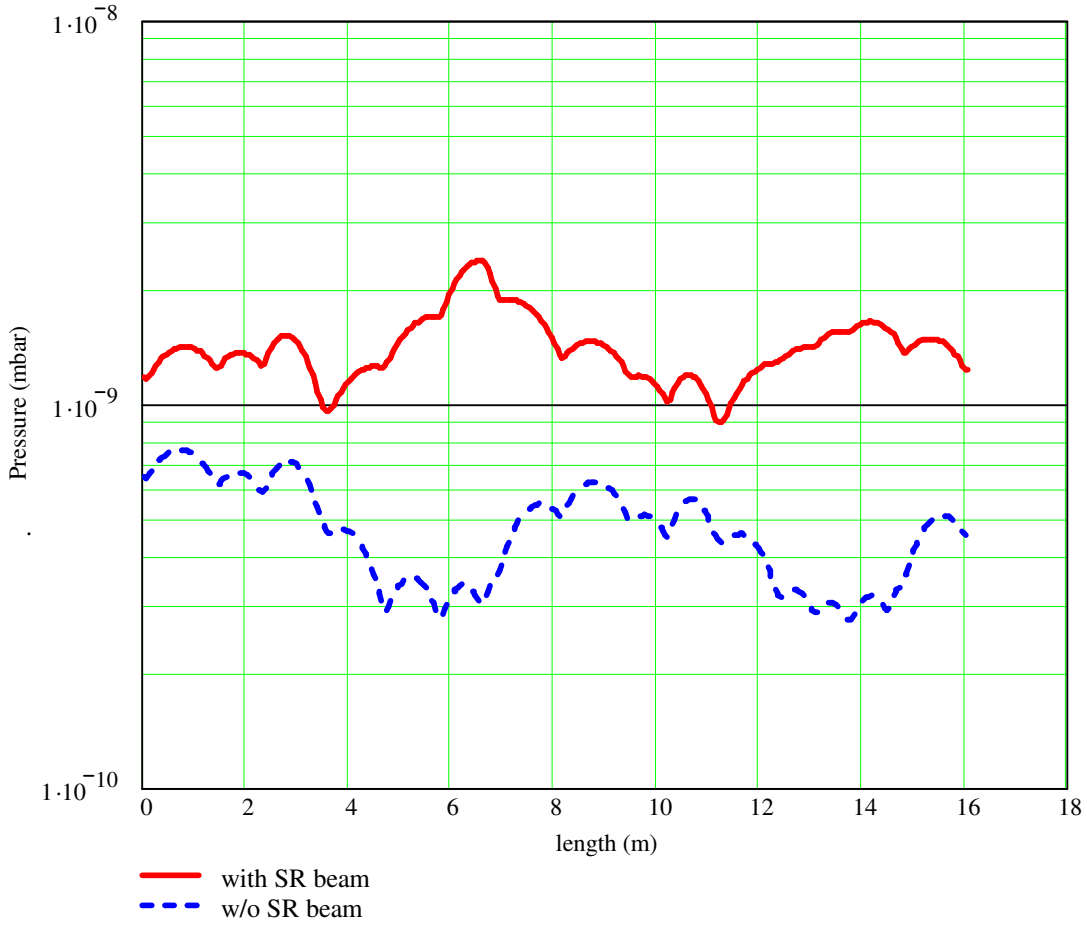

Figure 7.18: The Pressure profile for 1/8 of the storage ring, $P_{av,T} = 4.79\cdot10^{-10}$ mbar, $P_{av,PSD} = 9.4\cdot10^{-10}$ mbar, $P_{av}= 1.42\cdot10^{-9}$ mbar, at 2.0GeV, 200mA and at 200Ah.

In a following stage, another RF cavity will be installed, so SESAME will run at 2.2GeV and with a current of 300mA. Figure (7.19) shows the pressure profile under these conditions, the average dynamic pressure will be $1.61\cdot10^{-9}$ mbar at 500Ah, the average dynamic pressure increased even that the dose (cleaning effect) is more, the reason is due to the higher current and beam energy at this stage.

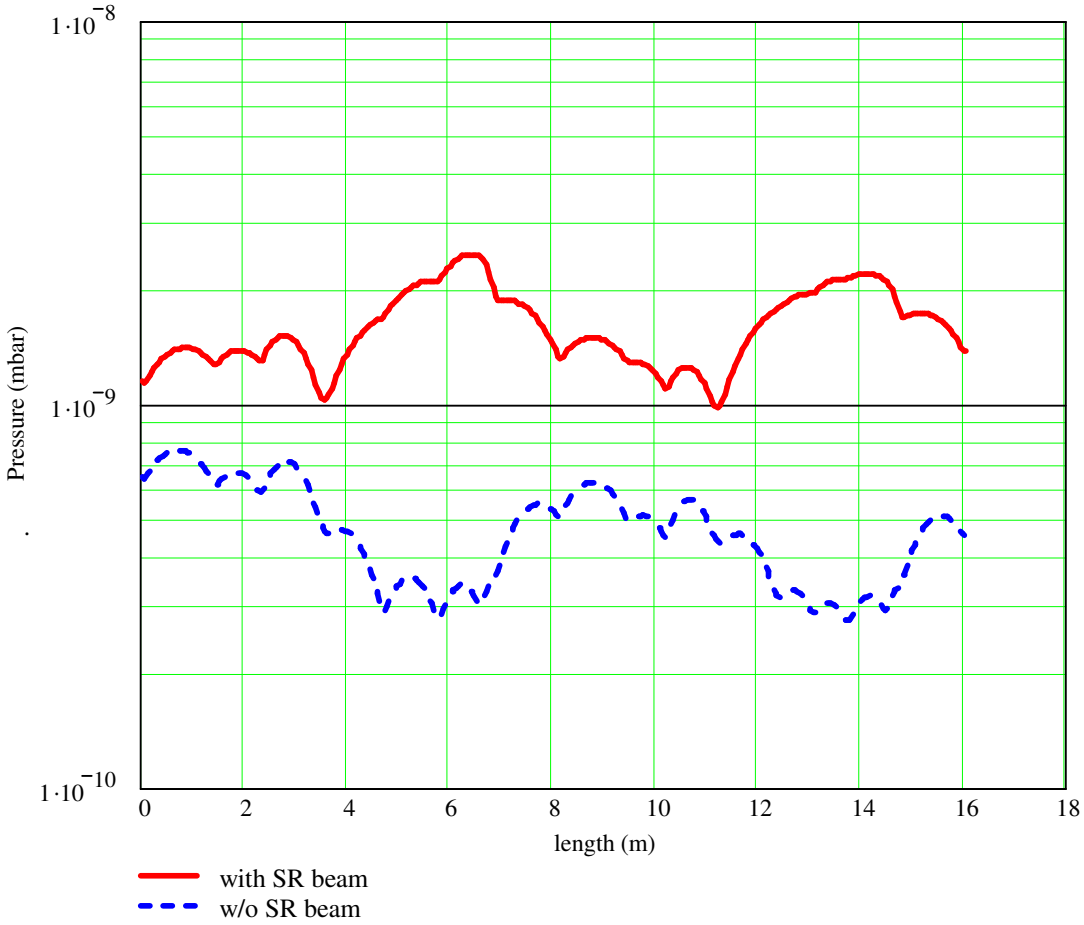

Figure 7.19: The Pressure profile for 1/8 of the storage ring, $P_{av,T} = 4.79 \cdot 10^{-10}$ mbar, $P_{av,PSD} = 1.13 \cdot 10^{-9}$ mbar, $P_{av} = 1.61 \cdot 10^{-9}$ mbar, at 2.2GeV, 300mA and at 500Ah.

In the following stage of the upgrade of the SESAME machine will be by having another RF cavity, as a result SESAME will run at 2.5GeV with a beam current of 350mA. Figure (7.20) shows the pressure profile under these conditions, the average dynamic pressure will be $1.79 \cdot 10^{-9}$ mbar at 800Ah.

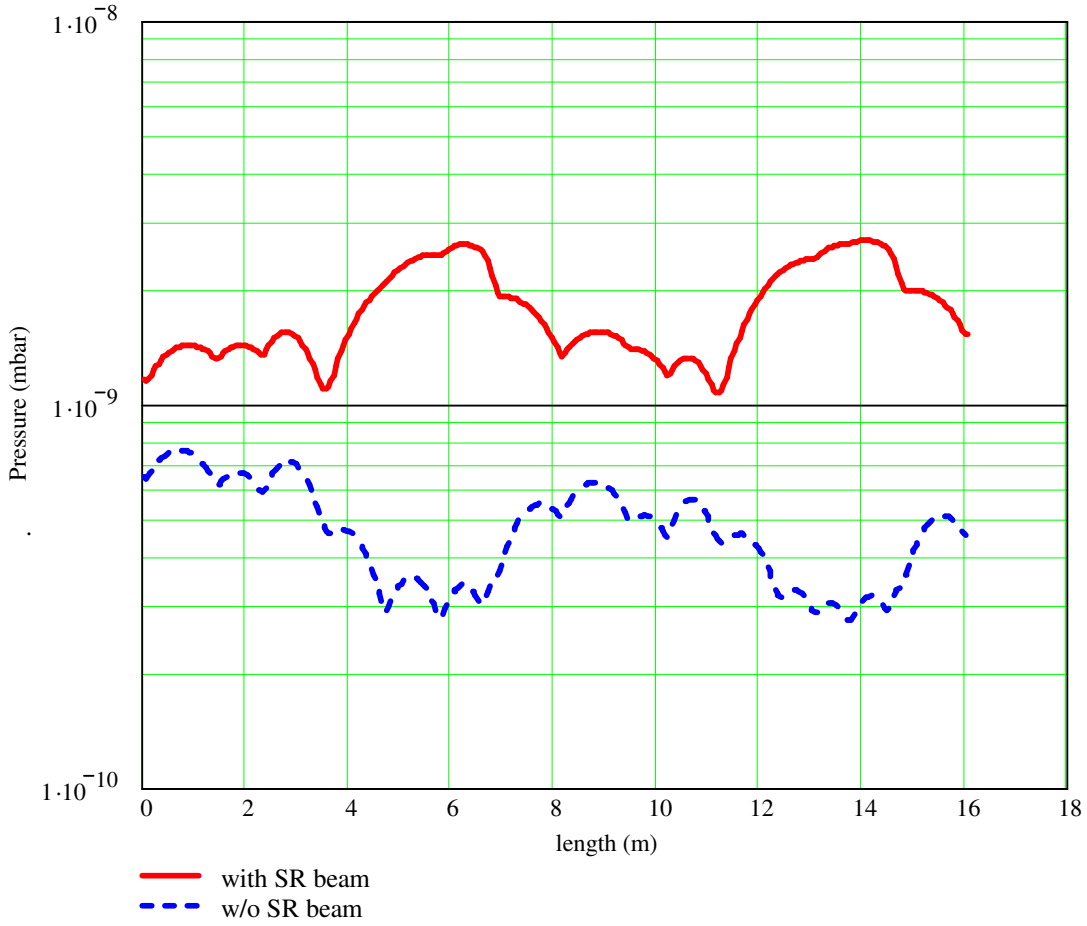

Figure 7.20: The Pressure profile for 1/8 of the storage ring, $P_{av,T}$ = 4.79·10^{-10} mbar, $P_{av,PSD}$ = 1.31 ·10^{-9} mbar, P_{av}= 1.79·10^{-9} mbar, at 2.5GeV, 350mA and at 800Ah.

Table (7.4) shows the expected average dynamic pressure values for different operational conditions (different beam energies, current and doses) for the same pumping speed for the pumps described in section 7.11.5.1.

It is important to point out that the beam doses indicated here are simply the multiplication of the current with the time (which the machine being operate under that specified current), and the beam energy is not considered, as for example (and roughly speaking), a vacuum chamber exposed to a dose of 100Ah at 2GeV is approximately equivalent to 70Ah or 80 Ah at 2.2GeV energy. It would be an approximation if the pressure considered for a certain current and dose to be the value for higher energies for the same current (for example, the pressure at 2.2GeV for 200mA at a dose of 500Ah in the table is 1.52·10^{-9} mbar, but for a more realistic value it could be the pressure value at 2.5GeV under the same conditions, i.e. 1.63·10^{-9} mbar).

These calculations were done to give a feeling of the values expected in the system and to optimise the location and the pumping speed of the pumps, but the actual value will depend in many factors that may not be expected until the machine being built.

Table 7.4: The variation of the average dynamic pressure (mbar) with the beam dose, beam energy and beam current.

Dose (Ah)	Beam Current = 200mA		
	2.0 GeV	2.2 GeV	2.5 GeV
Initial	$1.60\cdot10^{-6}$	$1.77\cdot10^{-6}$	$1.98\cdot10^{-6}$
100	$1.66\cdot10^{-9}$	$1.71\cdot10^{-9}$	$1.8\cdot10^{-9}$
200	$1.42\cdot10^{-9}$	$1.47\cdot10^{-9}$	$1.55\cdot10^{-9}$
300	$1.33\cdot10^{-9}$	$1.37\cdot10^{-9}$	$1.45\cdot10^{-9}$
400	$1.27\cdot10^{-9}$	$1.32\cdot10^{-9}$	$1.39\cdot10^{-9}$
500	$1.24\cdot10^{-9}$	$1.29\cdot10^{-9}$	$1.35\cdot10^{-9}$
600	$1.22\cdot10^{-9}$	$1.26\cdot10^{-9}$	$1.33\cdot10^{-9}$
700	$1.20\cdot10^{-9}$	$1.24\cdot10^{-9}$	$1.31\cdot10^{-9}$
800	$1.18\cdot10^{-9}$	$1.23\cdot10^{-9}$	$1.29\cdot10^{-9}$
900	$1.17\cdot10^{-9}$	$1.22\cdot10^{-9}$	$1.28\cdot10^{-9}$
1000	$1.16\cdot10^{-9}$	$1.21\cdot10^{-9}$	$1.27\cdot10^{-9}$

Dose (Ah)	Beam Current = 300mA		
	2.0 GeV	2.2 GeV	2.5 GeV
Initial	$2.31\cdot10^{-6}$	$2.5\cdot10^{-6}$	$2.77\cdot10^{-6}$
100	$2.17\cdot10^{-9}$	$2.25\cdot10^{-9}$	$2.38\cdot10^{-9}$
200	$1.81\cdot10^{-9}$	$1.89\cdot10^{-9}$	$2.0\cdot10^{-9}$
300	$1.67\cdot10^{-9}$	$1.74\cdot10^{-9}$	$1.85\cdot10^{-9}$
400	$1.59\cdot10^{-9}$	$1.66\cdot10^{-9}$	$1.77\cdot10^{-9}$
500	$1.54\cdot10^{-9}$	$1.61\cdot10^{-9}$	$1.71\cdot10^{-9}$
600	$1.51\cdot10^{-9}$	$1.57\cdot10^{-9}$	$1.67\cdot10^{-9}$
700	$1.48\cdot10^{-9}$	$1.55\cdot10^{-9}$	$1.65\cdot10^{-9}$
800	$1.46\cdot10^{-9}$	$1.52\cdot10^{-9}$	$1.62\cdot10^{-9}$
900	$1.44\cdot10^{-9}$	$1.51\cdot10^{-9}$	$1.60\cdot10^{-9}$
1000	$1.43\cdot10^{-9}$	$1.49\cdot10^{-9}$	$1.59\cdot10^{-9}$

Dose (Ah)	Beam Current = 350mA		
	2.0 GeV	2.2 GeV	2.5 GeV
Initial	$2.62\cdot10^{-6}$	$2.83\cdot10^{-6}$	$3.15\cdot10^{-6}$
100	$2.42\cdot10^{-9}$	$2.52\cdot10^{-9}$	$2.67\cdot10^{-9}$
200	$2.01\cdot10^{-9}$	$2.10\cdot10^{-9}$	$2.23\cdot10^{-9}$
300	$1.80\cdot10^{-9}$	$1.88\cdot10^{-9}$	$2.01\cdot10^{-9}$
400	$1.75\cdot10^{-9}$	$1.83\cdot10^{-9}$	$1.96\cdot10^{-9}$
500	$1.69\cdot10^{-9}$	$1.77\cdot10^{-9}$	$1.89\cdot10^{-9}$
600	$1.65\cdot10^{-9}$	$1.73\cdot10^{-9}$	$1.85\cdot10^{-9}$
700	$1.62\cdot10^{-9}$	$1.70\cdot10^{-9}$	$1.82\cdot10^{-9}$
800	$1.59\cdot10^{-9}$	$1.67\cdot10^{-9}$	$1.79\cdot10^{-9}$
900	$1.57\cdot10^{-9}$	$1.65\cdot10^{-9}$	$1.77\cdot10^{-9}$
1000	$1.56\cdot10^{-9}$	$1.63\cdot10^{-9}$	$1.75\cdot10^{-9}$

Dose (Ah)	Beam Current = 400mA		
	2.0 GeV	2.2 GeV	2.5 GeV
Initial	$2.92\cdot10^{-6}$	$3.16\cdot10^{-6}$	$3.5\cdot10^{-6}$
100	$2.70\cdot10^{-9}$	$2.79\cdot10^{-9}$	$3.0\cdot10^{-9}$
200	$2.20\cdot10^{-9}$	$2.30\cdot10^{-9}$	$2.46\cdot10^{-9}$
300	$2.01\cdot10^{-9}$	$2.11\cdot10^{-9}$	$2.26\cdot10^{-9}$
400	$1.91\cdot10^{-9}$	$2.00\cdot10^{-9}$	$2.14\cdot10^{-9}$
500	$1.84\cdot10^{-9}$	$1.93\cdot10^{-9}$	$2.07\cdot10^{-9}$
600	$1.79\cdot10^{-9}$	$1.89\cdot10^{-9}$	$2.02\cdot10^{-9}$
700	$1.76\cdot10^{-9}$	$1.85\cdot10^{-9}$	$1.98\cdot10^{-9}$
800	$1.73\cdot10^{-9}$	$1.82\cdot10^{-9}$	$1.95\cdot10^{-9}$
900	$1.71\cdot10^{-9}$	$1.80\cdot10^{-9}$	$1.93\cdot10^{-9}$
1000	$1.69\cdot10^{-9}$	$1.78\cdot10^{-9}$	$1.91\cdot10^{-9}$

7.11.6 The Effective Pumping Speed and the Design of the Pumping Ports

The results of the pressure profiles being shown before are for nominal and effective pumping speeds described in section 7.11.5.1, investigations need to be carried out to guarantee that the effective pumping speeds will be achieved by the system.

All the pumps are connected to the antechambers through pumping ports, as a result there is no need for a screen to separate the electron beam vacuum chamber from the pumping port (which is usually used to eliminate the interference between the circulating particles and the pumps), the shape of the pumping ports need to be designed carefully in order to guarantee the most from the pumping speed of the pumps, the effective pumping speed is limited by the transmission probability of the molecules through the pumping ports (i.e. the amount of molecules which will find their way to the pump from all molecules entering the pumping port).

By using Monte-Carlo simulation provided by MOLFLOW program [19], the transmission probability and the effective pumping speed of all the pumping ports of SESAME have been evaluated, table (7.5) shows the results of the transmission probability, conductance and the effective pumping speed at different nominal pumping speed for all SESAME pumping ports presented in chapter 5, for the pumping port types, see figure (7.16).

Table 7.5: the conductance and the effective pumping speed by the end of the pumping ports.

Pump location	Dia. (mm)	Width (mm)	Gap (mm)	Tr*	C** (L/s)	Effective Pumping Speed (L/s) for pumps with pumping speed of										
						75	100	150	200	300	400	500	600	800	900	1000
1,7 absorber	150	-	-	0.38	720	68	88	124	157	212	295	295	327	379	400	419
2, 4, 6, 9, 10 11 absorber	100	-	-	0.29	276	59	73	97	116	144	163	178	189	205	211	216
3, 8 absorber	150	-	-	0.33	688	68	87	123	155	209	253	290	-	-	-	-
Straight section pumps	100	-	-	0.28	258	66	84	116	144	190	-	-	-	-	-	-
1st pump at the dipole	-	300	15	0.14	73	37	42	49	52	58	-	-	-	-	-	-

* Transmission Probability.
** Conductance.

The following remarks are short discussion concerning the results shown in the previous table:

1- Almost all the pumps (except at the straight section and those located at absorber 1 and 7) are connected to the side of the antechamber through an elbow, but such a connection will reduce the conductance of the pumping ports and as a result the effective pumping speed of the pumps connected to them.
2- The pumping ports at the straight section have wide entrance and short pumping ports) as a result a good effective pumping speed can be achieved by using 150L/s pumps.
3- The first pump in the dipole vacuum chamber has the worst effective pumping speed, and from the results it is obvious that the spout has a conductance limitation (the effective pumping speed increases slightly with the increase of the pump pumping speed), the reason of that is that this pumping port had a small gap at the entrance and a narrow body and a long port, so the design need to be modified to get a larger conductance. Several modifications are reviewed here:
    I. A shorter pumping port by 40mm will increase the conductance to 84L/s and the effective pumping speed for 150L/s pump will increase from the old design to 54L/s.
    II. Opening out the pumping port to cover the space between the dipole poles, represented in figure (7.21) as “open port” will improve the conductance, different options for this design are shown in figure (7.22) and the results are represented in table (7.6).

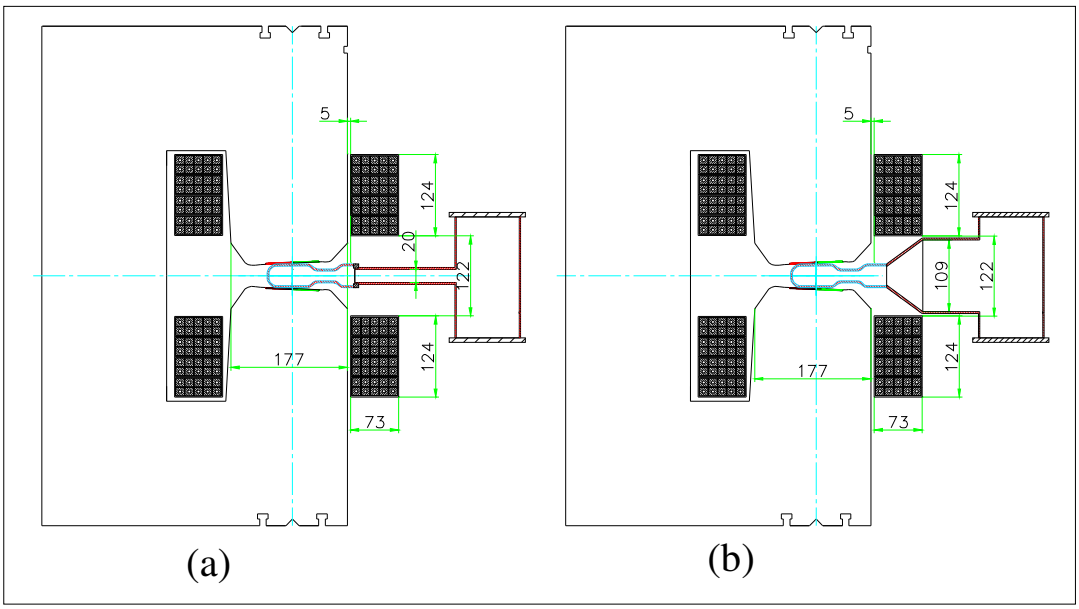

Figure 7.21: a. the current design of the pumping port of the first pump in the dipole vacuum chamber, b. the "open port" option.

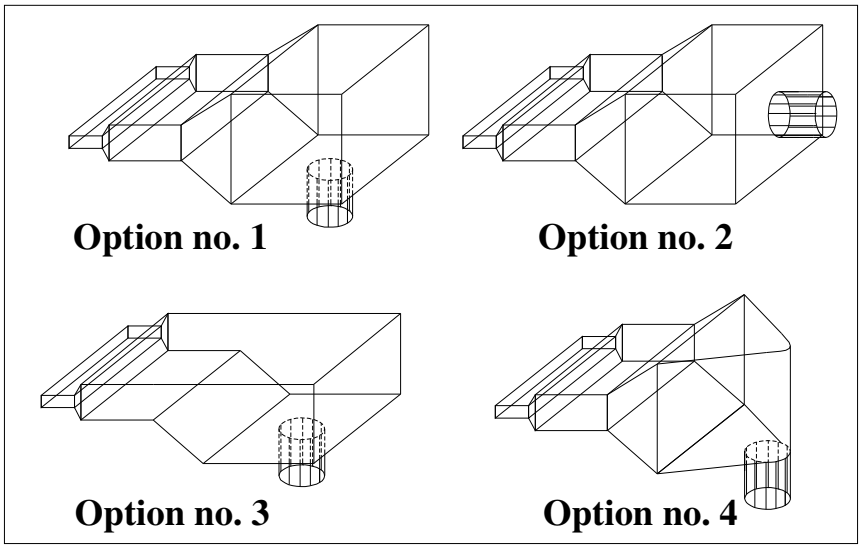

Figure 7.22: The different options available for the "open port" design.

Table 7.6: The conductance and the effective pumping speed by the end of the pumping ports for the different designs of the "open port" option.

Option no.	Tr	C (L/s)	Effective Pumping Speed (L/s) for pumps with pumping speed of	
			150	**200**
1	0.33	172	80	92.5
2	0.34	177	81.2	94
3	0.315	164	78	90
4	0.325	169	79	91.5

Taking into consideration the complication of the mechanical design of option no. 4 and that the lowest effective pumping speed is for option no. 3 and no. 4 in comparison with the other options, then these two designs must be discarded. Option no. 1 or 2, are the best in order to get the highest possible effective pumping speed, the limitation in achieving higher values, is due to the narrow gap of the entrance to the pumping port, which is not possible to change, the other solution to get higher effective pumping speed is by using a pump with higher pumping speed (200L/s or more) at this location, not only 150L/s.

7.12 SESAME Booster Synchrotron Vacuum System

BESSY I injection system will be upgraded to suit SESAME.

Figure (7.23) shows the different components of BESSY I injector vacuum system:

1. The booster synchrotron was divided into three sections by three gate valves, another gate valve was installed to isolate the microtron from the booster synchrotron.
2. Each straight section of the booster synchrotron had one getter ion pump (i.e. in total there were six ion pumps to pump down the booster synchrotron) one with 500L/s pumping speed and the others with 120L/s nominal pumping speed. In addition to these, an ion pump installed in the injection path, had been used to pump down the microtron.
3. Three turbomolecular pumps (each with 100L/s) were connected to the booster synchrotron for roughing down the system; another two were connected to the microtron. All were attached to the ring via isolating valves.
4. To measure the pressure around the booster synchrotron, the current from the ion pumps was monitored, also three high pressure gauges were distributed around the booster, another high pressure gauge and a low pressure gauge were installed to the microtron.

The pressure in the injection system must be in the acceptable ranges (below 10^{-7} mbar), the different components must be tested to guarantee that they are suitable for SESAME, for the ion pumps: leak tests, vacuum performance tests (pumping speed, outgassing rates) and other tests must be performed before being approved for SESAME use, general inspection of the pump body and the control units must be applied. For the gauges, the feed through must be inspected, how reliable they are, the readings variation in comparison with other new gauges and to the real pressure inside the system, the control units of the gauges need to be inspected to figure out how good they are for the use for SESAME.

It would be useful installing another pumps for the booster and the microtron, as the pressure used to be achieved during BESSY I operation was not low enough, also RGA and other vacuum equipment need to be installed to the injection system.

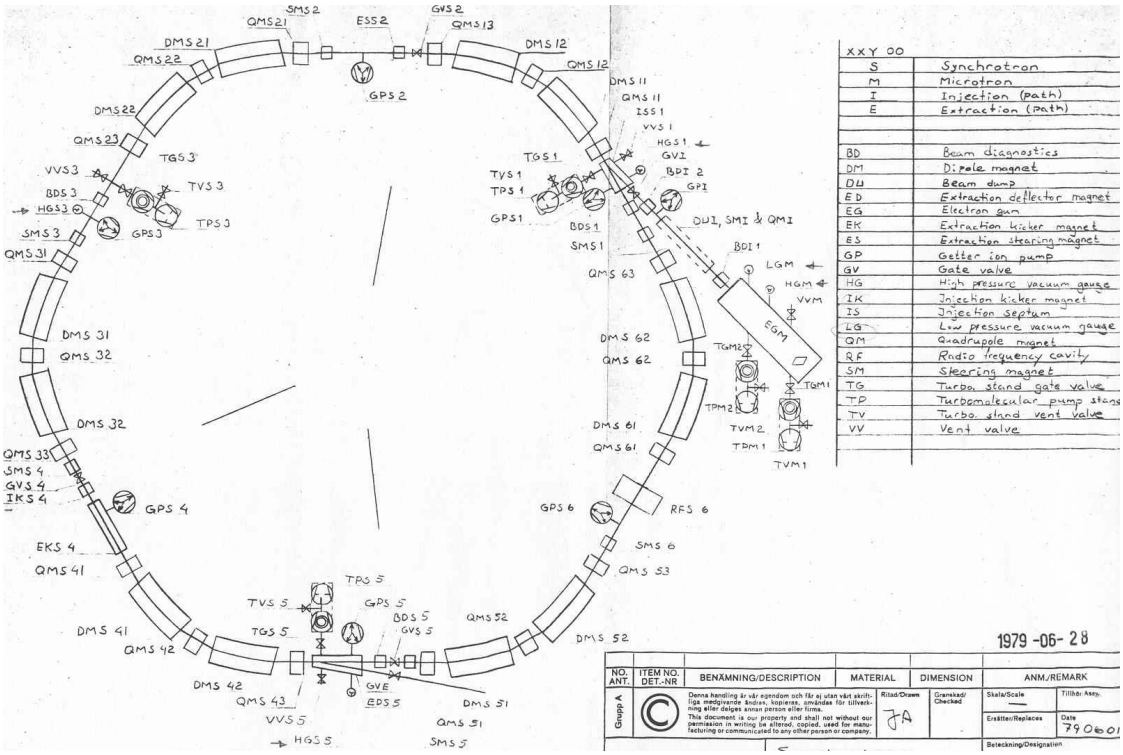

Figure 7.23: The vacuum system components of BESSY I injection system.

References:

[1] Oswala Grobner, *"Dynamic Outgassing"* CAS, 1999-Denmark.

[2] Ron Ried, "*Materials Choice for Diamond Vacuum System*", (Daresbury Laboratory Internal Report) Oct. 2000.

[3] Erhard Huttel, "*Materials for Accelerator Vacuum System*". CAS, 1999-Denmark.

[4] Lother Schulz, "*Stainless Steel Vacuum Chambers*" Oct. 2001.

[5] Keith Middleman, Daresbury Laboratory, Privet communication.

[6] SLS Handbook.

[7] D. Lowe, "*CLS Storage Ring Vacuum Chambers*", March 2001.

[8] Keith Middleman et al. *"Rough Pumping Systems for Diamond Storage Ring, Part 1 and Part 2"*, (Daresbury Laboratory Internal Report) Oct. 2001.

[9] Tom Weston, "*Capture pumps*", Vacuum Design Notes, Feb. 1996.

[10] Lothar Schulz, "*Sputter ion pumps*" CAS, 1999-Denmark.

[11] Diamond International vacuum workshop, Sep. 2002.

[12] *Diamond Synchrotron light source, Report of the design specifications",* June 2002.

[13] Joe Herbert, "*Vacuum Instrumentation for Diamond*", (Daresbury Laboratory Internal Report) Jan 2002.

[14] F. Daclon et al. *"Elettra Vacuum system, part 1"* July 1994.

[15] Ron Reid, "Cleaning for vacuum services", CAS, 1999-Denmark.

[16] Keith Middleman et al, *"Service Requirements for the Diamond Machine Complex"*, (Daresbury Laboratory Internal Report).

[17] Oleg Malyshev et al. *"Calculated Pressure profile Along the Diamond Storage Ring Cell."* (Daresbury Laboratory Internal Report) Jan 2002.

[18] Karl Jousten, *"Thermal Outgassing"* CAS, 1999-Denmark.

[19] Roberto Kersevan, MOLFLOW Program and MOLFLOW user guide, 1991.